

E × B Flow Effects on ITG Modes in Reverse Shear ASDEX Upgrade Discharges

A. Bottino, S.J. Allfrey, A.G. Peeters¹, O. Sauter, L. Villard and ASDEX Upgrade Team

*Centre de Recherches en Physique des Plasmas,
Association EURATOM - Confédération Suisse, EPFL, 1015 Lausanne, Switzerland*

¹ *Max-Planck Institut für Plasmaphysik, IPP-EURATOM Association,
D-85748 Garching bei München, Germany*

1. Introduction

Recent experiments with Internal Transport Barriers (ITB) have shown that the anomalous transport is considerably reduced by a radial electric field in the plasma [1]. Several theoretical models predict a strong stabilizing effect on toroidal Ion Temperature Gradient (ITG) modes due to the $\mathbf{E}_r \times \mathbf{B}$ flow. If the plasma rotation is sheared then a decorrelation in the mode structure appears, which tends to stabilize ITG modes. On the other hand, in some plasma discharges the shearing rate criterion does not predict a complete stabilization of the modes even if the criteria for identifying an ITB are satisfied.

In this paper we present a linear stability analysis for electrostatic microinstabilities in high confinement conditions by using the global electrostatic linear PIC code LORB5. This code can directly simulate the effect of the $\mathbf{E}_r \times \mathbf{B}$ drift induced by an imposed radial electric field. In particular we show results obtained using equilibria and equilibrium profiles of the ASDEX Upgrade discharge 13149 in which an Ion Internal Transport Barrier (ITB) was identified. This discharge has a reverse shear configuration and a relatively strong radial electric field.

2. The model

The code LORB5 follows the linear time evolution of quasi-neutral electrostatic perturbations of the local Maxwellian distribution function in a 2D magnetic configuration. In LORB5 the ion dynamic is described by a gyrokinetic model derived by Hahm [2] based on a Vlasov-Poisson system in which the fast ion cyclotron motion has been averaged out. Trapped electrons are modeled using drift-kinetic equations, no finite electron Larmor radius effects are retained. Passing electrons are supposed to respond adiabatically to the perturbation. The time evolution of the perturbed ion distribution function $\tilde{f} = f - f_0$ is given by:

$$\frac{\partial \tilde{f}}{\partial t} + \dot{\mathbf{R}} \cdot \nabla \tilde{f} + v_{\parallel} \frac{\partial \tilde{f}}{\partial v_{\parallel}} = -\frac{\langle \mathbf{E} \rangle \times \mathbf{h}}{B^*} \frac{\partial f_0}{\partial \mathbf{R}} - \frac{q_i \langle \mathbf{E} \rangle}{m_i} \cdot \mathbf{h} \frac{\partial f_0}{\partial v_{\parallel}} - \left(v_{\parallel} \frac{\partial f_0}{\partial v_{\parallel}} + \frac{1}{2} v_{\perp} \frac{\partial f_0}{\partial v_{\perp}} \right) \langle \mathbf{E} \rangle \cdot \frac{\mathbf{h} \times \nabla \mathbf{B}}{B^{*2}}$$

Where $\langle \mathbf{E} \rangle$ represents the gyro-averaged perturbed electric field, $B^* = B + (m_i v_{\parallel} / q_i) \mathbf{h} \cdot \nabla \times \mathbf{h}$ and $(\mathbf{R}, v_{\parallel}, v_{\perp}, \alpha)$ are the guiding center variables. The $\mathbf{E}_r \times \mathbf{B}$ drift velocity $\mathbf{u} = (-\nabla \phi_0 \times \mathbf{B}) / B^2$, with a given $\phi_0(\psi_p)$, modifies the unperturbed guiding center trajectories:

$$\begin{aligned} \dot{\mathbf{R}} &= v_{\parallel} \mathbf{h} + \mathbf{u} \left[1 - \frac{1}{\Omega} \mathbf{h} \cdot \nabla (\mathbf{u} + v_{\parallel} \mathbf{h}) \right] + \frac{1}{\Omega} \mathbf{h} \times [v_{\parallel} \nabla \times (\mathbf{u} + v_{\parallel} \mathbf{h}) \times \mathbf{h} + \\ &\quad + \mu \nabla B + \frac{1}{2} \nabla u^2] \\ \dot{v}_{\parallel} &= -\mathbf{h} \cdot [\mu \nabla B + \frac{1}{2} \nabla u^2] - \mathbf{u} \cdot [\mathbf{h} \times \nabla \times (\mathbf{u} + v_{\parallel} \mathbf{h})] \end{aligned}$$

For small Mach numbers of the $\mathbf{E}_r \times \mathbf{B}$ drift velocity \mathbf{u} , terms of order $(u/v_{thi})^2$ and $\epsilon_B (u/v_{thi})$ can be neglected. The model is closed by a quasi-neutrality equation valid up to $k_{\perp} \rho_L \simeq 2$ [3]:

$$\begin{aligned} (1 - \nabla_{\perp} \frac{T_i}{m_i \Omega^2} \nabla_{\perp}) (\tilde{n}_i - \tilde{n}_e) &= \nabla_{\perp} \cdot \left(\frac{n_0}{B \Omega} \nabla_{\perp} \phi \right) \\ \tilde{n}_e &= n_0 (1 - \alpha_b) \frac{e \phi}{T_e} + \int_{trapped} B^* \delta(\mathbf{R} + \rho - \mathbf{x}) \tilde{f}_e d\alpha d\mu dv_{\parallel} d\mathbf{R} \\ \tilde{n}_i &= \int \tilde{f}(\mathbf{R}, v_{\parallel}, \mu) \delta(\mathbf{R} - \mathbf{x} + \rho) d^6 z \end{aligned}$$

The code LORB5 is coupled with the MHD equilibrium code CHEASE [4].

3. Results

Equilibrium profiles for the ASDEX UPGRADE discharge 13149 are shown in Figure 1. The radial electric field has been computed using a force balance equation.

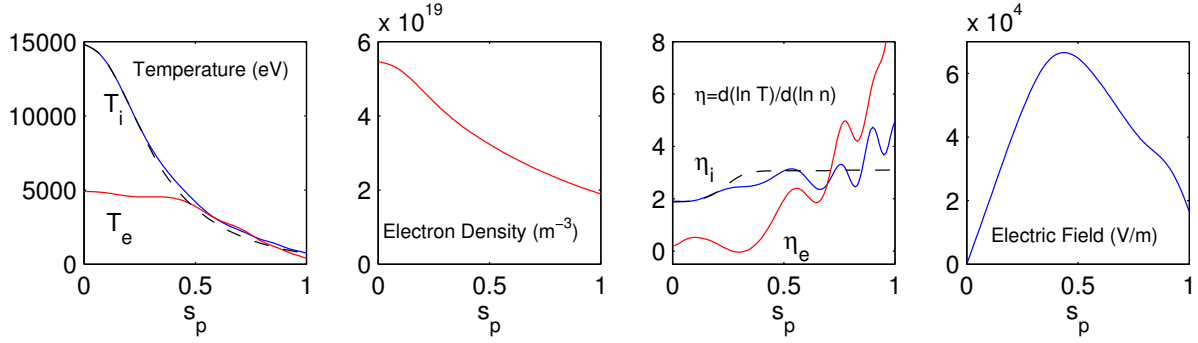


Figure 1. *Interpolated experimental profiles for electrons (red) and ions (blue) as a function of $s_p = \sqrt{\psi_p/\psi_{p,edge}}$. Black dashed lines correspond to a flat η_i profile.*

In this shot the main contribution to the force balance comes from the $(v_\varphi B_\theta)$ term. Figure 2 shows the complete spectrum of the most unstable modes in the absence of applied radial electric field for fully adiabatic and drift-kinetic trapped electrons. Trapped electron dynamics further destabilize the mode but the frequency is still in the ion diamagnetic direction, therefore the dominant electrostatic mode is an ITG. Moreover, this equilibrium is unstable even when a $\eta_i(s_p) = 0$ profile is used, in this case the instability is driven by trapped electrons and the modes are pure Trapped Electron Modes (TEM). All the ITG modes tend to be localized in the region where the shear is positive and where the η_i profile has a local maximum. In Figure 3 we see that for $n = 40$ there are two modes growing with comparable growth rate, localized around $s_p = 0.55$ and $s_p = 7.3$, corresponding to the first two bumps of the η_i profile. We performed another set of simulations using a flat η_i profile (black dashed lines in Figures 1 and 2). The corresponding ion temperature profile is still inside the experimental error bars. Local bumps on the η_i profile do not affect the global behavior of the system: the growth rate and the mixing length estimate for the diffusion coefficient of the most unstable modes are very close to the previous ones. The radial position of the modes increases linearly with n . The applied radial electric field has a strong stabilizing effect even with trapped electrons and it is strong enough to completely stabilize ITG modes. Figure 4 shows that for $n = 30$ the ITG mode becomes stable for values of the Mach number lower than the experimental one.

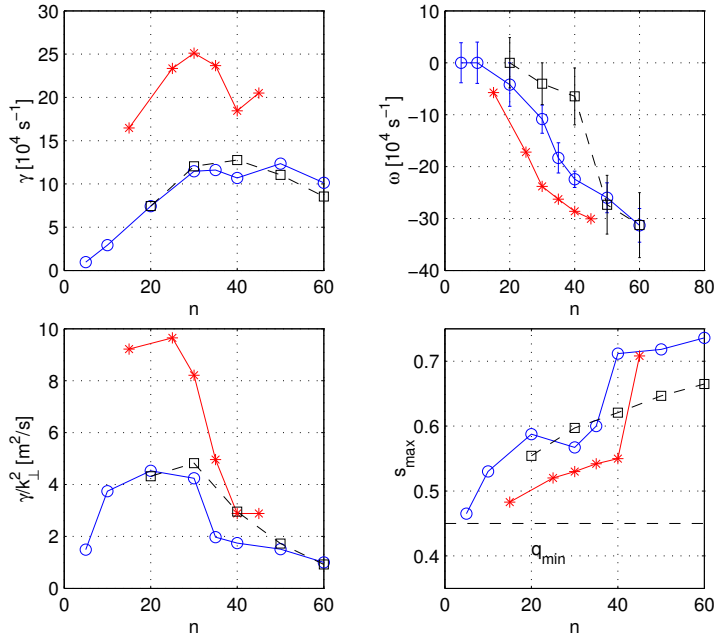


Figure 2. *Growth rates (a), real frequency (b), mixing length estimation of χ (c) and radial position (d) for fully adiabatic (blue circles) and trapped (red stars) drift-kinetic electrons. Black squares correspond to flat η_i profile, adiabatic electrons.*

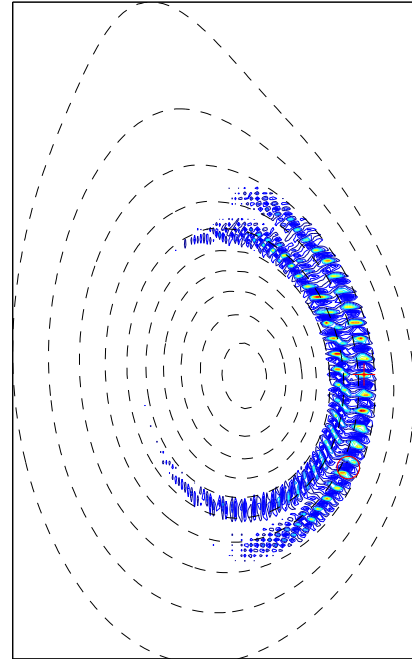


Figure 3. *Poloidal plot of the perturbed electric potential for $n = 40$, adiabatic electrons, interpolated T_i profile.*

It must be underlined that, linearly, both the local shear and the local value of u , combined with the magnetic shear, contribute to the stabilization [5]. In our simulations we see that a non-zero local value of the $\mathbf{E}_r \times \mathbf{B}$ flow shifts away the maximum of the mode amplitude from the unfavorable ∇B region [6]. This effect is supposed to be less important in the non-linear phase, where the turbulent behavior of the system breaks the ballooning structure of these modes.

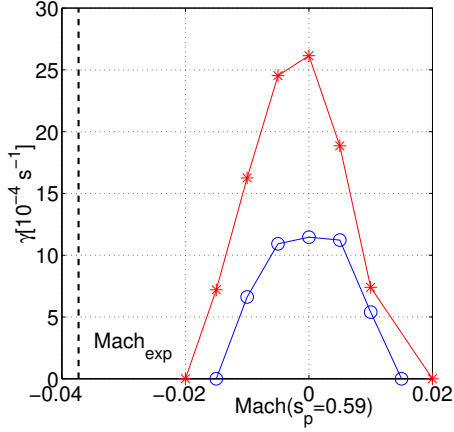


Figure 4. Mach number scan, $n = 30$, for fully adiabatic (blue circles) and trapped (red stars) electrons, $Mach(s_p = 0.59)_{exp} = -0.037$.

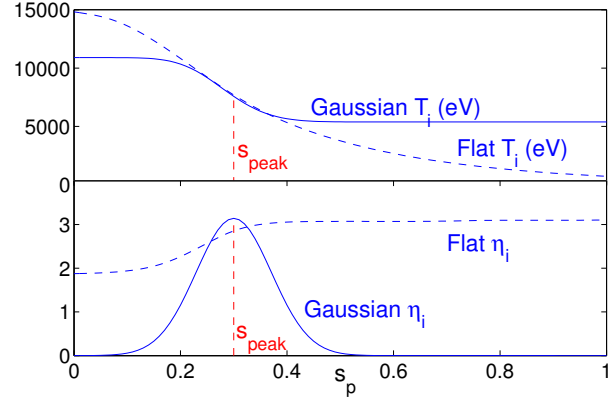


Figure 5. Gaussian η_i profile centered at $s_{peak} = 0.3$ and corresponding T_i profile, $\tau(s_{peak}) = \tau(s_{peak})_{exp}$.

In order to study the behavior of the system in the negative shear region, we have produced local ion temperature profiles. The corresponding η_i profile is a Gaussian having an amplitude comparable with the maximum value of the flat η_i profile, $\eta_i(s_{peak}) \simeq 3.2$. The Gaussian width has been chosen larger than the average radial extension of the mode $n = 30$, flat η_i profile. An example of a Gaussian centered in $s_p = s_{peak} = 0.3$ is given in Figure 5. By displacing the center of the Gaussian along the minor radius we get informations about the local stability of the system. Results for fully adiabatic electrons are summarized in Figure 6, black squares. When the Gaussians are centered in the positive shear region we find modes that have growth rates very close to the global ones. In the negative shear region this magnetic configuration allows for unstable modes but they are much less unstable.

In the negative shear region the ratio $\tau(s_p) = T_e(s_p)/T_i(s_p)$ becomes small while it stays close to unity outside q_{min} . It is well known that small values of τ have a strong stabilizing effect on ITG modes. Another set of simulations has been performed by setting for each Gaussian profile $\tau(s_{peak}) = 1$ (Figure 6, red circles).

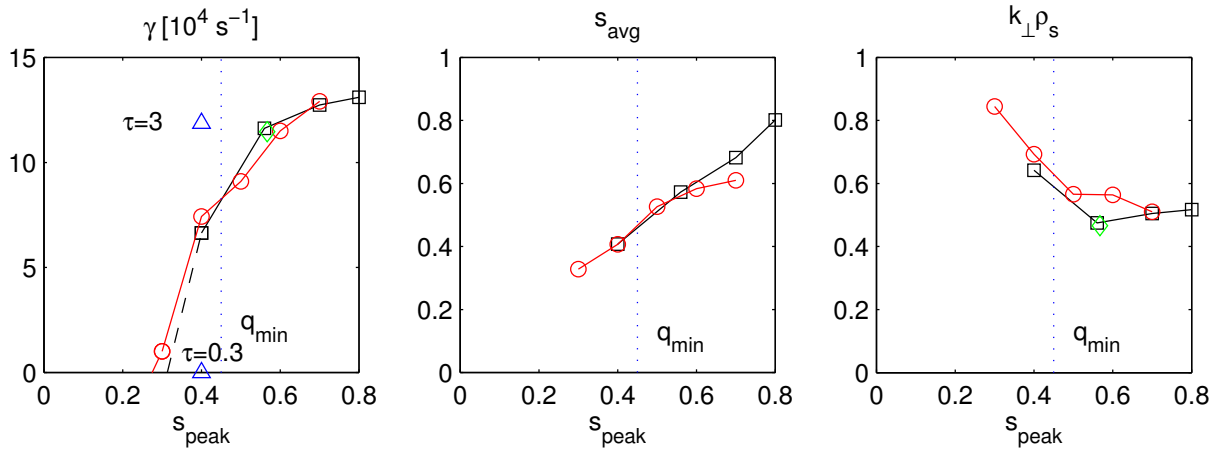


Figure 6. Growth rate (a), radial position (b) and $k_{\perp} \rho_s$ (c) of the most unstable modes as a function of s_{peak} for $\tau(s_{peak}) = \tau(s_{peak})_{exp}$ (black squares) and $\tau(s_{peak}) = 1$ (red circles). Green diamonds, flat η_i profile. Blue triangles, Gaussian profile, $s_{peak} = 0.4$, $\tau(0.4) = 0.3$ and $\tau(0.4) = 3$.

The experimental value of τ contributes to the stabilization, but it is not strong enough to justify the observed behavior inside q_{min} . The effect of τ can be seen in Figure 6 (blue triangles): $\tau(s_{peak}) = \tau(0) \simeq 0.3$ completely stabilize the ITG mode for $s_{peak} = 0.4$, while the growth rate doubles with $\tau(s_{peak}) = 3$.

The reversed shear configuration itself plays a role in the stabilization. We have produced a new set of equilibria with different q profiles by changing the current profile and keeping the plasma shape and the total current ($I_P \simeq 1MA$) constant (Figure 7). These q profiles are equivalent for $s_p > 0.5$, therefore the results obtained with global profiles are essentially the same. When local T_i profiles, with $\tau(s_{peak}) = 1$, are used (Figure 8) the growth rates obtained with flat or monotonic safety factor profiles show the usual weak linear dependence in the aspect ratio and unstable modes are found down to $s_p \simeq 0.2$. Therefore these two magnetic configurations are much more unstable, for $s_p < q_{min} \simeq 0.45$, than the reverse shear experimental equilibrium. Those modes tend to become slab-like and to have a narrow radial extension and their contribution to the transport could be weak. Trapped electron dynamics can further destabilize these modes. Therefore a similar local analysis will be performed using local T_e profiles and including trapped electrons in the simulation.

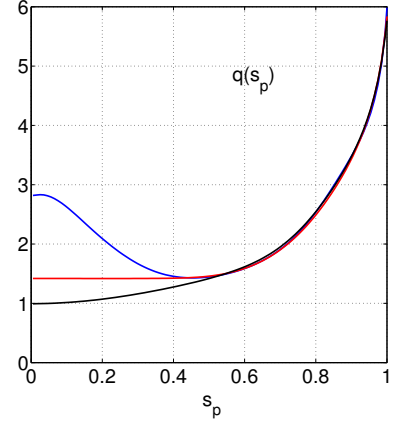


Figure 7. Experimental q profile (blue), flat (red) and monotonic (black) q profiles, constant total current ($I_P \simeq 1MA$)

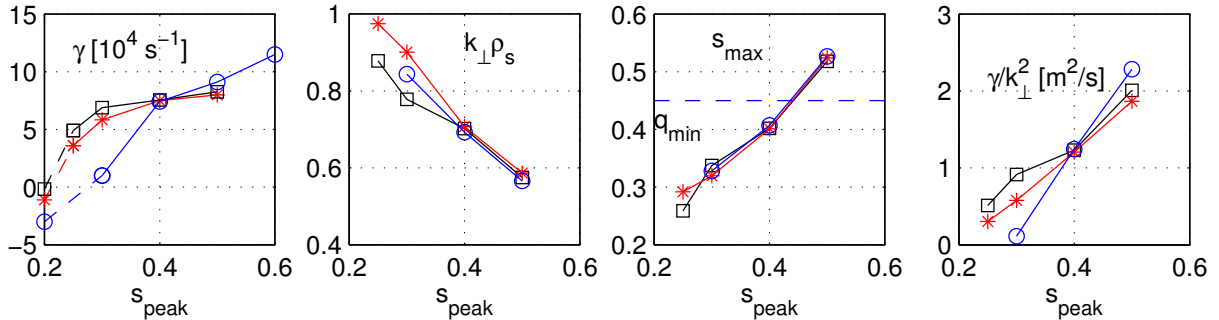


Figure 8. Growth rate (a), $k_{\perp}\rho_s$ (b), radial position (c) and mixing length estimation of χ (d), $\tau(s_{peak}) = 1$, for flat (red stars), monotonic (black squares) and reversed (blue circles) q profiles.

4. Conclusions

The ASDEX Upgrade discharge 13149 is linearly stable when the equilibrium radial electric field is taken into account. Without electric field, the global mode spectrum shows that the most unstable modes are ITG modes, localized in the positive shear region. Unstable modes can be found inside q_{min} , when local η_i profiles are used, albeit with smaller growth rates. In addition to the $\mathbf{E}_r \times \mathbf{B}$ flow, we conclude that at least two other physical mechanisms contribute to stabilize these modes: the reverse shear profile and, to a lesser degree, the local value of τ .

This work was partly supported by the Swiss National Science Foundation. Simulations were performed on the parallel servers SGI Origin 3800 and SWISS-T1 of the Ecole Polytechnique Fédérale de Lausanne.

References

- [1] K.H. Burrell, Phys. Plasmas **3**, 4658 (1996)
- [2] T.S. Hahm, Phys. Plasmas **3**, 4658 (1996)
- [3] A. Bottino et al., Theory of Fusion Plasmas, Int. Workshop, Varenna, 2000, 327
- [4] H. Luetjens, A. Bondeson and O. Sauter, Comput. Phys. Commun. **97**, 219 (1996)
- [5] L. Villard, A. Bottino and O. Sauter, Phys. Plasmas **9**, (to appear in June 2002)
- [6] M. Maccio, J. Vaclavik and L. Villard, Phys. Plasmas **8**, 895 (2001)